



*Supplement of*

## **Projecting end-of-century climate extremes and their impacts on the hydrology of a representative California watershed**

**Fadji Z. Maina et al.**

*Correspondence to:* Fadji Z. Maina ([fadjizaouna.maina@nasa.gov](mailto:fadjizaouna.maina@nasa.gov))

The copyright of individual parts of the supplement might differ from the article licence.

## Supplement A: Comparisons between VR-CESM simulations and PRISM

Figure S1 illustrates the Variable Resolution Community Earth System Model (VR CESM) grid for (a) globe and (b) coastal western US with the Cosumnes watershed overlaid in dark gray.

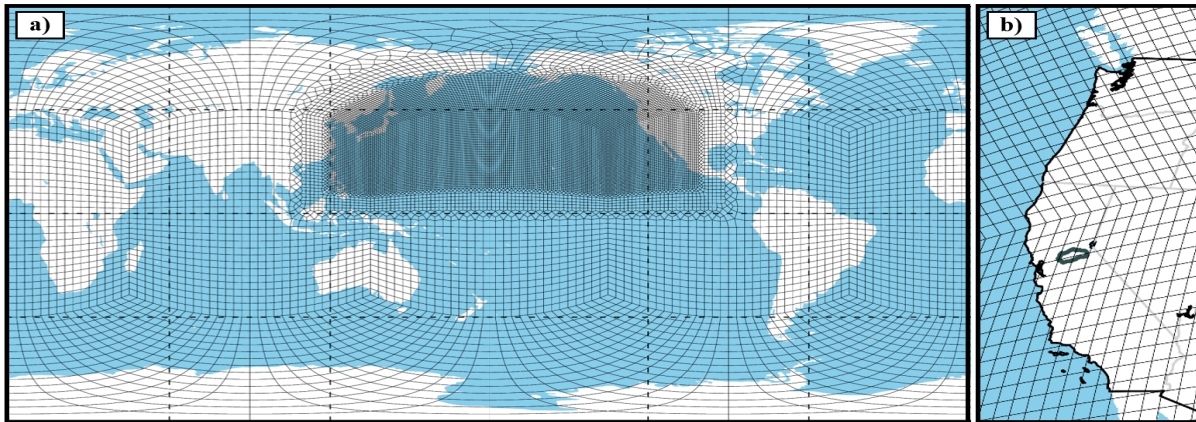


Figure S1: Variable Resolution Community Earth System Model (VR CESM) grid for (a) globe and (b) coastal western US with the Cosumnes watershed overlaid in dark gray.

To identify if VR-CESM is fit for purpose to simulate historical dry, median, and wet WYs, and inform potential biases in future projections, we first conduct a model comparison to a widely used observational product, the Parameter-elevation Relationships on Independent Slopes Model (PRISM; Daly et al., 2008) at 4 km resolution analogous to Rhoades et al., (2020a). However, in this study, we focus our assessment of VR-CESM fidelity over California and the Cosumnes watershed. PRISM precipitation and temperature data spanning 1981-2019 are compared with the VR-CESM 1985-2015 simulations. We note that a mismatch in the time period (1981-2019 versus 1985-2015) is deliberate. As stated previously, VR-CESM is simulated under AMIP-protocols, and therefore we do not expect VR-CESM to exactly recreate past historical WYs. However, we do expect that our 30-year simulation can reasonably recreate the range of WY types over

California and the Cosumnes, which is why we utilize the broader range of PRISM WYs that are available.

Figure S2 highlights differences in dry, median, and wet WY accumulated precipitation relative to the 1981-2019 PRISM climatology. VR-CESM generally recreates the spatial pattern of anomalous dry and wet patterns across California for each WY type. This is shown via the common regions of minimum and maximum anomalies relative to the PRISM climatology. Notably, there are regions where VR-CESM anomalies are not consistent with PRISM. This is primarily shown in the wettest water year in portions of the Central Valley, western slopes of the Sierra Nevada, and southern California. This is likely correlated with resolution and the lack of orographic gradients (both valleys and peaks) in VR-CESM at 28km resolution. Mismatches in accumulated precipitation may also be due to representation of atmospheric rivers (ARs) in VR-CESM that were found to be generally larger, slightly more long-lived and make landfall more frequently over California (Rhoades et al., 2020b). Figure S3 shows Cosumnes watershed WY accumulated precipitation and surface temperature. WY accumulated precipitation is shown in Figure S3a and 2b for PRISM and VR-CESM, respectively. All WY accumulated precipitation simulated by VR-CESM over 1985-2015 are within the range in PRISM, save for the wettest WY. This is shown more explicitly in quadrant space in Figure S3c where the range of annual bias in VR-CESM relative to the range of interannual variability in PRISM for accumulated precipitation and temperature is shown. VR-CESM generally simulates a wetter historical period over the Cosumnes (range of bias of 1330 mm) relative to PRISM (range of interannual variability of 1320 mm). Basin-average minimum (421 mm) and maximum (1740 mm) WY accumulated precipitation are slightly larger than is found in PRISM. Of relevance to this study, PRISM has shown notable uncertainties in the Sierra Nevada. Lundquist et al., 2015 showed that an

underrepresentation of the most extreme storm total precipitation in the Sierra Nevada can result in an upper-bound uncertainty of 20% in WY accumulated precipitation. Therefore, the wettest WY of VR-CESM is well within the 20% uncertainty range of PRISM's wettest WY ( $1580 \pm 316$  mm). Further, differences in basin-average WY accumulated precipitation between VR-CESM and PRISM are non-significant using a t-test and assuming a p-value  $< 0.05$ . The range of temperature bias in VR-CESM ( $2.74$  °C) relative to the range of PRISM interannual variability ( $2.93$  °C) was also within the temperature uncertainties discussed in Strachan and Daly, 2017. They showed that a general cool-bias in PRISM temperatures were found on the leeward side of the Sierra Nevada when compared with 16 out-of-sample in-situ observations across an elevation gradient of 1950 to 3100 meters with an overall mean bias of  $-1.95$  °C (maximum temperature) and  $-0.75$  °C (minimum temperature).

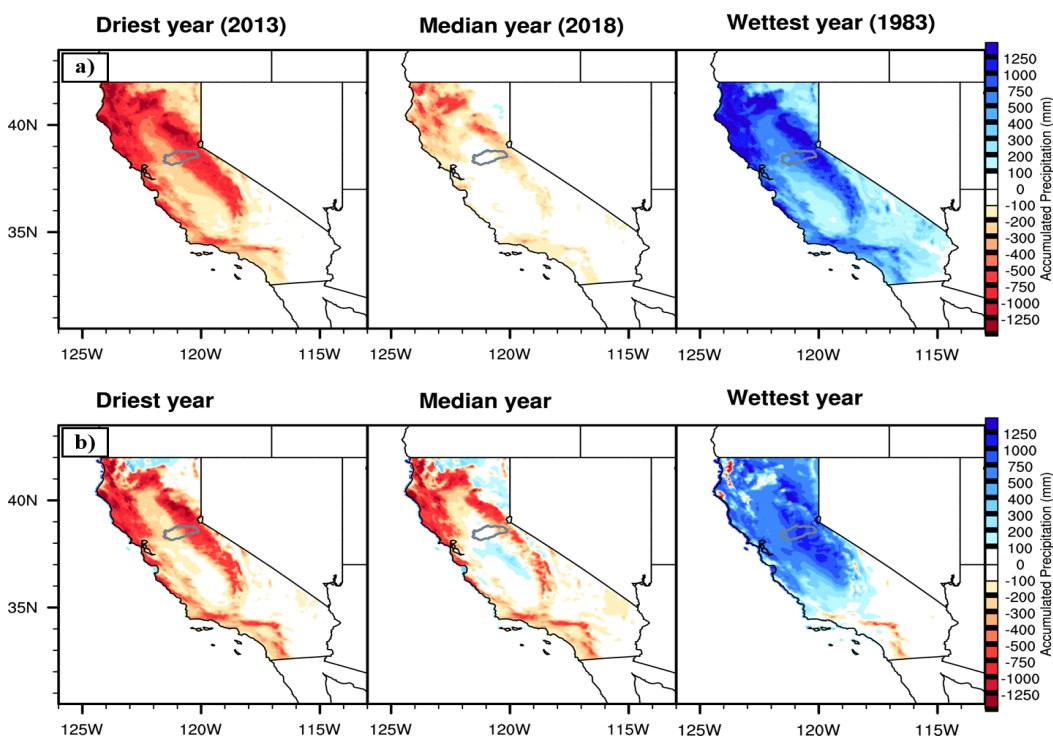


Figure S2: Differences in the driest, median, and wettest water year accumulated precipitation over California in a) PRISM and b) VR-CESM relative to the 1981-2019 PRISM climatology. The Cosumnes watershed boundary is outlined in gray.

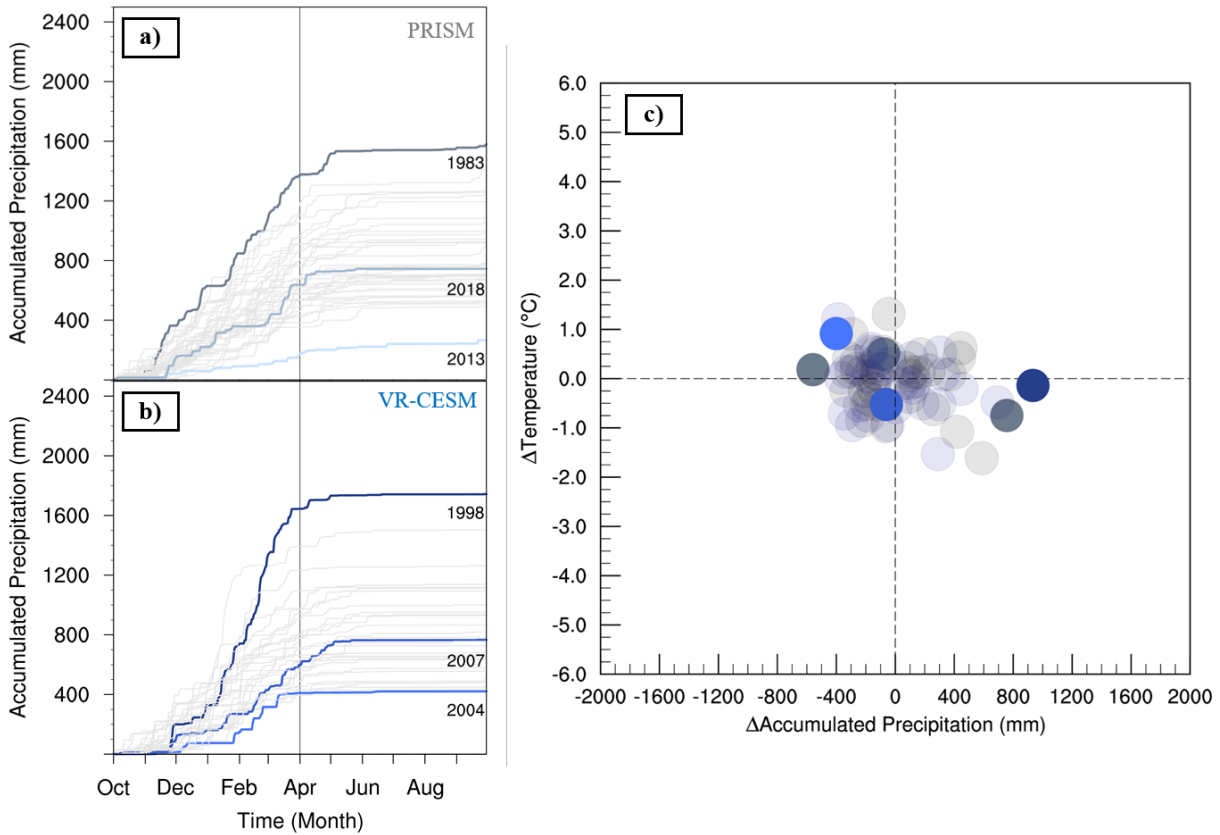


Figure S3: Cosumnes watershed accumulated precipitation totals in a) PRISM (gray; 1981-2019) and b) VR-CESM (blue; 1985-2015) with dry, median, and wet years emboldened. c) shows differences in PRISM (gray) and VR-CESM (blue) relative to the PRISM climatology (1981-2019) in temperature and accumulated precipitation quadrant space. Dry, median, and wet water years are emboldened.

## Supplement B: Integrated Hydrologic Model Parameterization

### 1. Input Variables

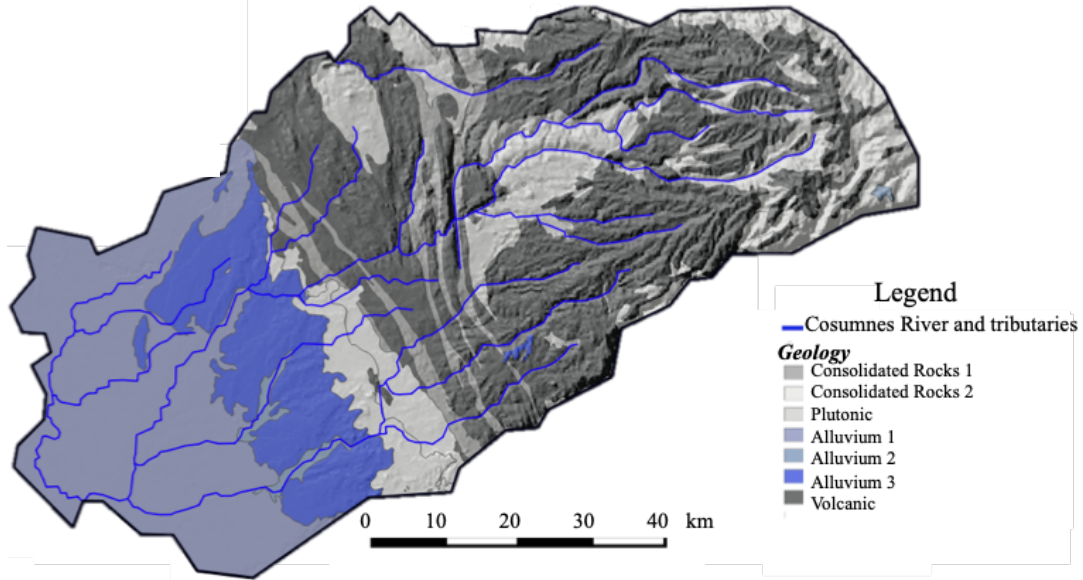


Figure S4: Geological map of the Cosumnes watershed (source: USGS, Jennings et al., 1977)

Hydrodynamic properties based on the geology				
Geological Formation	Porosity (-)	Specific Storage ( $m^{-1}$ )	Van Genuchten $\alpha$ ( $m^{-1}$ )	Van Genuchten $n$ (-)
Bedrock (Consolidated, Plutonic and Volcanic Rocks)	0.02	$10^{-6}$	3.0	3.0
Alluvial aquifers	0.2	$10^{-4}$	3.0	3.0

Table S1: Assigned values of hydrodynamic parameters (porosity, specific storage and Van Genuchten parameters). Values are based on literature review (Faunt et al., 2010; Faunt and Geological Survey (U.S.), 2009; Flint et al., 2013; Gilbert and Maxwell, 2017; Welch and Allen, 2014).

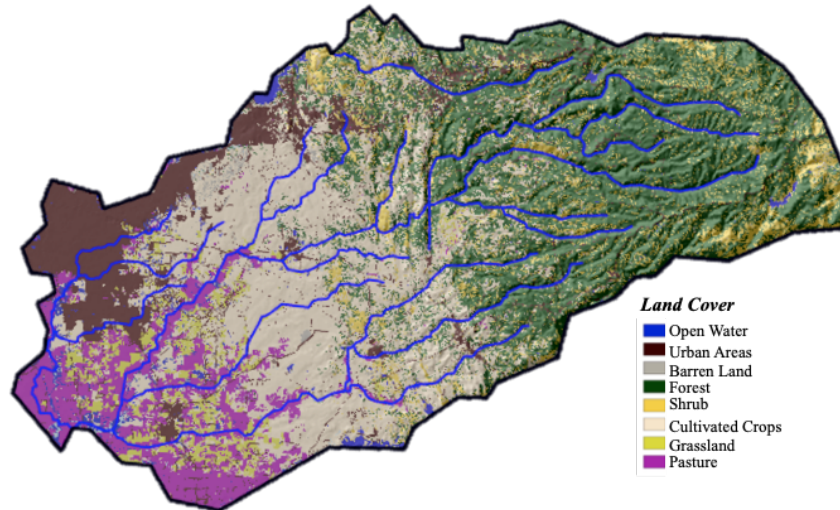


Figure S5: Cosumnes watershed characteristics: land use and land cover (source: Homer et al., 2015), and model boundaries.

Surface roughness based on land use			
Land Use	Manning Coefficient ( $\text{h.m}^{-1/3}$ )		
Forest	$5 \times 10^{-2}$		
Shrub land and agricultural area	$5 \times 10^{-3}$		
Urban areas	$5 \times 10^{-5}$		
Crop properties			
Crop Type and Reference	Height (m)	Maximum Leaf Area Index (-)	Minimum Leaf Area Index (-)
Alfalfa (Evelt et al., 2000; Orloff, 1995; Robison et al., 1969)	0.6	6.0	2.0
Pasture (Buermann et al., 2002; King et al., 1986; Rahman and Lamb, 2017)	0.12	6.0	1.0
Vineyards (Johnson and Pierce, 2004; Vanino et al., 2015)	0.9	3.0	0.6

Table S2: Manning coefficients and crop properties

Boundary conditions	Value
Mokelumne and American river	Weekly-varying Dirichlet boundary conditions. These values are based on the measured river stages.
Sierra Nevada limit	No flow Neumann boundary condition
Bottom of the model	No flow Neumann boundary condition

Table S3: boundary conditions

## 2. Numerical model set-up

Domain size	~7000 km <sup>2</sup>								
Spatial discretization	200 m horizontal from 0.1 m to 30 m in the vertical direction								
	Vertical Resolution								
	Layer	1	2	3	4	5	6	7	8
$\Delta z(m)$	0.1	0.3	0.6	1.0	8.0	15.0	25.0	30.0	
Simulation time	Model validation (from water year 2012 to water year 2017), then future water years								
Temporal discretization	hourly								

Table S4: Numerical model discretization

### 3. Output variables

<b>Selected output variables</b>	<b>Temporal scale</b>	<b>Spatial scale</b>
Snow Water Equivalent	Yearly, monthly, and hourly	Domain-average and point scale
Evapotranspiration	Yearly, monthly, and hourly	Domain-average and point scale
Soil Moisture	Yearly, monthly, and hourly	Domain-average and point scale
River Stages (also surface water storages)	Yearly, monthly, and hourly	Domain-average and point scale
Groundwater levels variations (also subsurface storages)	Yearly, monthly, and hourly	Domain-average and point scale

Table S5: Selected output variables

## Supplement C: Integrated Hydrologic Model Validation

We compared temporal variations of streamflow at 3 stations located in the Sierra (uplands), the intersection between the Sierra and the Central Valley, and the outskirts of Sacramento (see Figure S6). Four wells in the watershed (see Figure S6) have reasonable, publicly available records of groundwater levels and were used to check the ability of the model to reproduce water table depth variations.

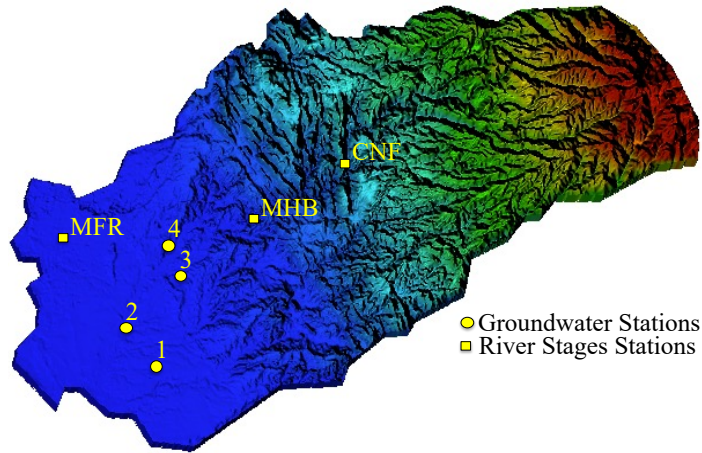


Figure S6: The locations of the 3 streamflow gauges (CNF, MHB, and MFR) and 4 groundwater wells (stars).

Figure S7a depicts the comparisons between simulated and measured river stages at the 3 stations indicated in Figure S6. Absolute errors (L1) in m and relative errors (L2) are shown in Table S6. Differences between simulated and measured streamflow vary between 0.4 and 0.8 m (Table S6) indicating that the model is able to reproduce the river dynamics.

Absolute differences given by:

$$L_{1i,j} = |X_{mes_{i,j}} - X_{sim_{i,j}}| \quad (C1)$$

Where  $L_{1,i,j}$  is the absolute difference associated with cell  $i$  and time  $j$ ,  $X_{mes,i,j}$  is the measured (or remotely sensed) data, and  $X_{sim,i,j}$  the simulated value.

Relative differences  $L_{2,i,j}$  are given by:

$$L_{2,i,j} = \frac{|X_{mes,i,j} - X_{sim,i,j}|}{X_{mes,i,j}} \quad (C2)$$

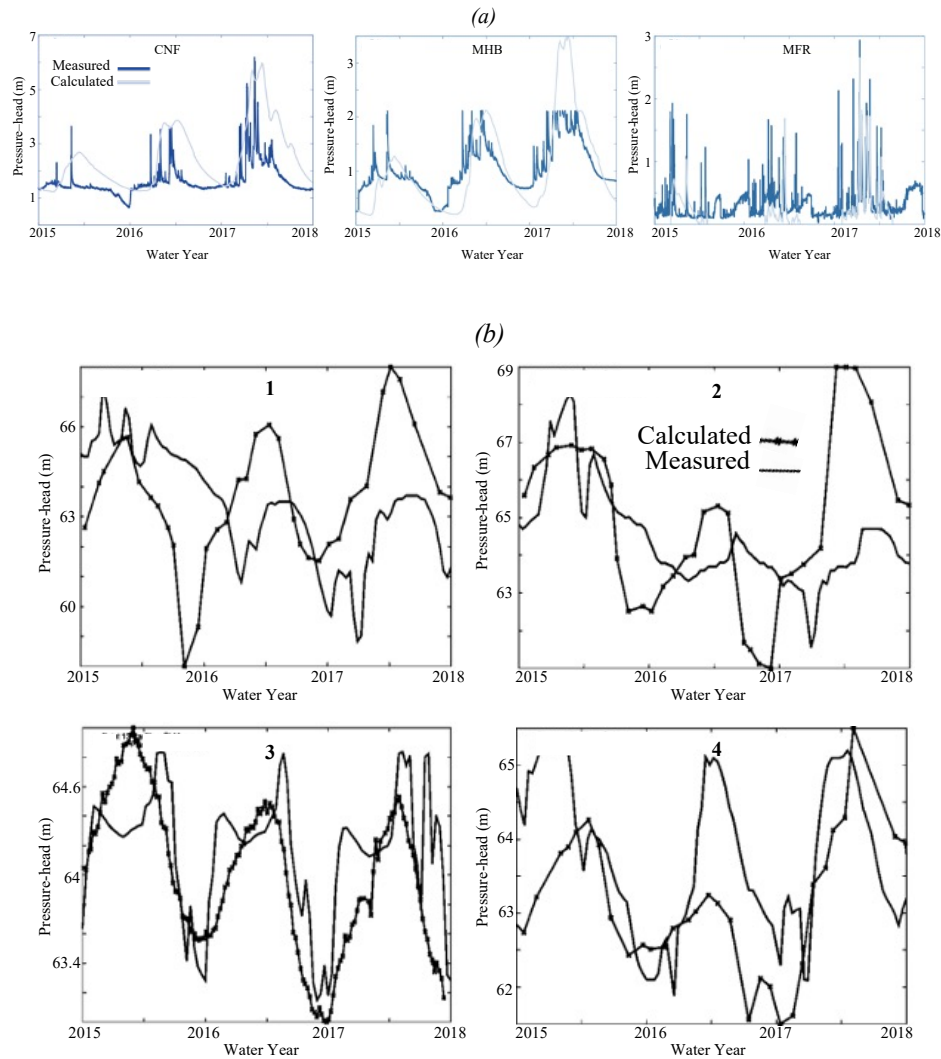


Figure S7: Comparisons between measured and calculated (a) river stages (i.e., pressure-heads simulated by ParFlow-CLM) and (b) subsurface pressure-head. The location of the selected points is indicated in Figure S6.

<b>Measurements</b>	<b>L<sub>1</sub> (m)</b>	<b>L<sub>2</sub> (-)</b>
River Stages (CNF)	0.8	0.5
River Stages (MHB)	0.4	0.36
River Stages (MFR)	0.57	1.06
Groundwater Levels (Well 1)	3.73	0.05
Groundwater Levels (Well 2)	1.63	0.02
Groundwater Levels (Well 3)	0.476	0.0077
Groundwater Levels (Well 4)	1.08	0.016

Table S6: Differences between measured and calculated surface and groundwater levels. L<sub>1</sub> is the absolute error and R<sub>2</sub> the relative error.

Comparisons between simulated and calculated groundwater levels (here referred to as the pressure-heads at the bottom of the domain) shown in Figure S7b indicate that the model has reasonable agreements with measurements. As shown in Table S6, the error varies between 0.47 to 3.73 m depending on the station. Mismatches between simulated and observed groundwater levels at wells 1 and 2 are likely due to an inaccurate estimation of pumping in these areas. The temporal variations of the groundwater levels show an impact of withdrawals but because these withdrawals are hard to estimate the model isn't correctly reproducing these trends.

ParFlow-CLM also solves the key land surface processes governing the transfer of water and energy at the land-atmosphere-soil interface: evapotranspiration, snow dynamics, and soil moisture. In Maina et al., (2020a), rigorous comparisons between the ParFlow-CLM simulated land surface processes and remotely sensed estimates of these variables were conducted (Figure

S8). Table S7 shows the correlation coefficient between ParFlow-CLM results and the various datasets compared.

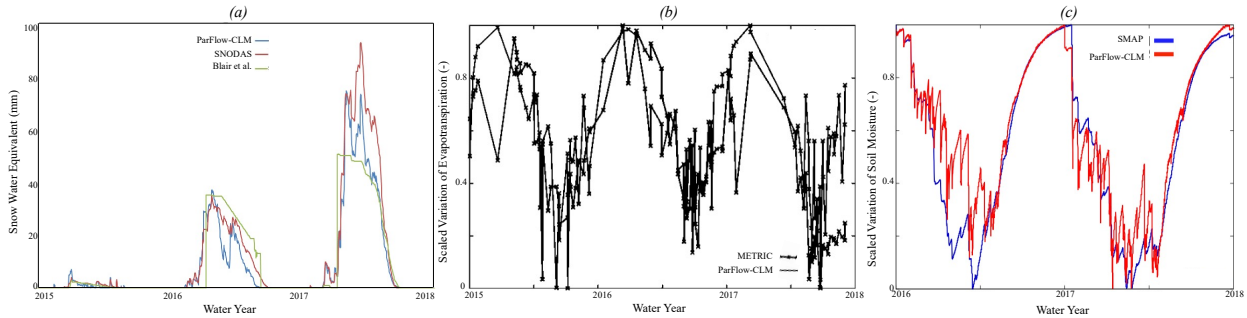


Figure S8: (a) Comparisons between domain-averaged total snow water equivalent obtained with ParFlow-CLM, SNODAS and Bair et al., reconstruction, (b) Comparisons between actual evapotranspiration obtained with ParFlow-CLM and METRIC (c) Relative variation of soil moisture obtained with ParFlow-CLM and SMAP. Note that the x-axis of (c) is shorter because of the availability of SMAP data

Satellites based products	L <sub>1</sub> (m)	L <sub>2</sub> (-)	Pearson Correlation Coefficient
SWE SNODAS (mm)	3.09	3.77	0.97
SWE Bair et al., (mm)	3.80	2.69	0.84
Soil Moisture SMAP (-)	0.217	3.07	0.94
ET METRIC (mm/s)	0.067	1.40	0.6

Table S7: differences between measured and remotely sensed evapotranspiration (METRIC), soil moisture (SMAP), and snow water equivalent (SNODAS and Bair et al., 2016)